Asian Journal of Pure and Applied Mathematics

Volume 6, Issue 1, Page 132-155, 2024; Article no.AJPAM.1463

Richardson Extrapolation Technique for Singularly Perturbed Parabolic Convection-diffusion Problems with a Discontinuous Initial Condition

Desta Sodano Sheiso [a*]

[a] *Department of Mathematics, Indian Institute of Technology Guwahati, Guwahati - 781 039, India.*

Author's contribution

The sole author designed, analyzed, interpreted and prepared the manuscript.

Article Information

Open Peer Review History:
This journal follows the Advanced Open Peer Review policy. Identity of the Reviewers, Editor(s) and additional Reviewers, peer review comments, different versions of the manuscript, comments of the editors, etc are available here: https://prh.globalpresshub.com/review-history/1463

Received: 11/12/2023

Accepted: 15/02/2024

Published: 27/03/2024

Original Research Article

Abstract

This article presents the Richardson extrapolation techniques for solving singularly perturbed parabolic convection-diffusion problems with discontinuous initial conditions (DIC). The scheme uses backward-Euler for temporal derivatives on a uniform mesh and classical upwind finite difference method (FDM) for spatial derivatives on a piecewise-uniform (Shishkin) mesh. This scheme provides almost a first-order convergence solution in both space and time variables. The method employs an upwind finite difference operator on a piecewise- uniform mesh to approximate the gap between the analytic function and the parabolic issue solution. The numerical solution's accuracy is improved by using Richardson extrapolation techniques, which raises it from $O(N^{-1}\ln N + \Delta t)$ to $O(N^{-2}\ln^2 N + \Delta t^2)$ in the discrete maximum norm, where N is the number of spatial mesh intervals, and Δt is the size of the temporal step size. Parameter-uniform error estimates, stability results, and bounds for the truncation errors are all addressed. Finally, numerical experiments are presented to validate our theoretical results.

**Corresponding author: E-mail: desta.sodano@iitg.ac.in, destasodano2010@gmail.com;*

Keywords: Singularly perturbed parabolic problems; Upwind scheme; discontinuous initial condition; interior layer; Richardson extrapolation technique; Piecewise-uniform Shishkin mesh.

2010 Mathematics Subject Classification: AMS 65M06, 65M12, 65M15.

1 Introduction

This article will delve into a particular type of problem called singularly perturbed parabolic convection-diffusion problems, which exhibit interior layers caused by discontinuous initial conditions [1, 2, 3, 4]. These concerns are pertinent across various engineering and applied mathematical domains, including convection-dominated flows in fluid dynamics, quantum mechanics, elasticity, chemical reactor theory, gas porous electrodes theory, as well as heat and mass transfer in chemical and nuclear engineering. Our investigation is rooted in the studies conducted by Gracia *et al.* [5] and [6] in the field of numerical analysis. The paper introduces an analytical function that aligns with discontinuous initial conditions and solves a differential equation with constant coefficients. The interior layer function's position evolves in the convection-diffusion problem, requiring tracking techniques like the Shishkin mesh. An explicit discontinuous function $S(x,t)$ captures the discontinuous initial conditions-related singularity, and asymptotic expansions for the solution $u(x,t)$ are constructed. Subtracting this singular function yields $y(x,t) = u(x,t) - S(x,t)$, the solution of singularly perturbed parabolic convection-diffusion problems. In real applications, we Use the Richardson extrapolation technique for singularly perturbed parabolic convection-diffusion problems with a DIC to predict the diffusion rate of the reactant's effects on the performance of the polymer electrolyte membrane fuel cell. In addition, an analytical approach is being investigated to study the impact of gas channel draft angle on PEMFC performance and species distribution. In [7, 8, 9], studied singularly perturbed reaction-diffusion problems in which discontinuities existed in either the boundary or the initial condition. Here, we expand this approach to address a convection-diffusion problem with discontinuous initial conditions. This introduces a time-dependent shift in the position of the internal layer arising from the initial condition discontinuity. These types of problems arise in several branches of engineering and applied mathematics, including convection-dominated flows in fluid dynamics, quantum mechanics, elasticity, chemical reactor theory, gas porous electrodes theory, heat, and mass transfer in chemical and nuclear engineering, etc.[10, 11]. In [9], we introduce an alternative numerical algorithm that incorporates a coordinate transformation designed to align the mesh with the interior layer location, allowing us to handle this more general case effectively. The linearized Navier-Stokes equations at high Reynolds numbers, heat transport problems with large Péclet numbers, and magneto-hydrodynamic duct problems at Hartman numbers are well-known examples of singularly perturbed problems (SPPs) [10, 11, 12, 13].

Classical numerical methods, as acknowledged in [11, 12, 13, 14], prove ineffective in approximating solutions of SPPs. Moreover, as ε approaches zero, standard finite difference or finite element schemes on uniform meshes fall short in handling singularly perturbed differential equations (SPDE) with continuous data. As evident from the literature cited above, most researchers aim to discover a numerical solution for singularly perturbed parabolic convection-diffusion problems. Nevertheless, this paper presents an innovative methodology by creating and assessing parameter-uniform numerical techniques, employing piecewise-uniform meshes tailored for a specific category of singularly perturbed parabolic convection-diffusion problems with DIC. Consequently, the development of parameter-uniform numerical methods aligns with a well-established principle in the exploration of numerical solutions for SPPs.

Several researchers, such as Clavero et al. [7, 15, 16], Kopteva [8], and Shishkin [7, 17], have developed algorithms for singularly perturbed parabolic convection-diffusion problems with uniform second-order convergence in both variables. The problem involves initial conditions with discontinuities, resulting in interior and boundary layers. For parabolic problems, the initial layer's location evolves in convection-diffusion scenarios but remains fixed in reaction-diffusion cases. The interior layer moves along a characteristic curve related to the reduced problem in the considered model. Gracia and O'Riordan [6, 8, 9] have investigated the interior layer's movement in convection-diffusion SPPs, while Shishkin [18] studied parabolic SPPs with piecewise smooth initial data using finite difference grids. Gracia and O'Riordan [9, 19, 20] established a parameter-uniform numerical method for

problems with incompatible boundary and initial data. Recent academic interest focuses on efficient methods for singularly perturbed parabolic convection-diffusion problems through Richardson extrapolation. Numerous authors have utilized this technique to enhance convergence order, albeit at increased computational complexity [13]. O'Riordan *et al.* [21] combined implicit Euler with the classical upwind finite difference operator on a piecewise uniform mesh in one dimension, achieving first-order parameter-uniform convergence in both space and time variables.

Richardson extrapolation is a well-known technique used by many authors to enhance the order of convergence with a cost of higher computational complexity. Using an error after extrapolation decomposition, we employ a Richardson extrapolation technique, as demonstrated by several authors [22, 23], to yield a more precise numerical solution for the model problem with DIC. This strategy has been employed by numerous writers to achieve higher-order convergence compared to conventional numerical methods. Natividad and Stynes [23] used the technique for a two-point boundary value problem in one dimension. Das and Natesan [1] used this for higher-order convergence for delay parabolic SPPs and 2D parabolic convection-diffusion problems on Shishkin mesh. Academic publications show a technique achieving higher-order convergence compared to classical numerical schemes for singularly perturbed convection-diffusion problems using Shishkin meshes, extensively explored by Gracia, Clavero, as evidenced by citations like [5, 23, 13, 24, 25, 17, 18]. Mukherjee and Natesan derived the best error estimates for the upwind technique on Shishkin-type meshes, specifically addressing singularly perturbed parabolic problems with discontinuous convection coefficients [13]. M. Natividad and M. Stynes [23, 13] have discussed the application of Richardson extrapolation to convection-diffusion problems using Shishkin meshes. Shishkin *et al.* [24, 25] developed parameter-uniform numerical methods for singularly perturbed parabolic problems with DIC terms, using fitted operator techniques instead of upwind FDM operators.

In this paper, we look at a group of singularly perturbed parabolic convection-diffusion problems that generate solutions with internal layers as a result of DIC. Existing literature proposes various methods to address these issues. To gain a comprehensive understanding of these techniques, we recommend consulting the book by Farrell et al.'s [10, 11], farrell2000robust and Röös *et al.*'s work [13]. M. Pickett and G. Shishkin [17] employed parameter-uniform finite differences to solve singularly perturbed parabolic diffusion-convection-reaction problems. For a more in-depth exploration of numerical treatments of SPPs, reference the works cited in [12, 14], including works by Clavero, Miller, and Shishkin [15, 26, 7], Farrell, Hegarty, Miller, O'Riordan, and Shishkin, Röös, Stynes, and Tobiska [11, 12, 14, 27, 18].

With this motivation, the Richardson extrapolation method for improving the accuracy of numerical solutions in one-dimensional singly perturbed parabolic convection-diffusion problems with discontinuous beginning conditions (2.1). This method improves the order of accuracy for SPPs by focusing on fundamental upwind finite difference techniques. We demonstrate enhanced accuracy for basic upwind finite difference schemes within the SPP class dealing with discontinuous initial circumstances by using asymptotic expansion approaches to establish exact restrictions for the continuous solution and its derivatives. This method effectively approximates both temporal and spatial derivatives, boosting the implicit upwind finite difference method's convergence from nearly first-order to nearly second-order.

The rest of the article is organized as follows: Section 2 defines a continuous problem using a transformation to fix the interior layer's position in time, providing solution decomposition, derivatives, and discontinuous initial conditions-defined singular function. Section 3 introduces a numerical scheme in the transformed domain based on a classical implicit upwind scheme and establishes a parameter-uniform error bound. Section 4 discusses the Richardson extrapolation technique and determines the error estimate for the extrapolated discrete problem. Section 5 we present numerical examples to validate the theoretical results. The paper concludes with the conclusions.

Notations: The domains are represented by $\Omega = (0,1), \quad \tilde{d} = \tilde{d}(0), \quad D = \Omega \times (0,T)$. In this paper, C is a constant independent of both the singular perturbation parameter ε and all discretization parameters. The jump of a function ϕ at a discontinuity point $\tilde{d}$ is defined as:

$$[\phi](\tilde{d}) = \phi(\tilde{d}^+) - \phi(\tilde{d}^-).$$

We denote the maximum norm over any region $||.||_{\bar{D}}$, which is defined by $||u||_{\bar{D}} = \max_{x\in\bar{D}} |u(x,t)|$, $(x,t) \in D$ for any function u.

The space $C^{0+\gamma}(D)$ where $D \subset \mathbb{R}^2$, denotes an open set and is defined by

$$C^{n+\gamma}(\mathrm{D}) = \left\{ z : \frac{\partial^{i+m} z}{\partial x^i \partial y^m} \in C^{0+\gamma}(\mathrm{D}), \quad \forall i, m \in \mathbb{N} \cup \{0\} \text{ and } \quad 0 \le i + 2m \le n \right\}, \quad n \ge 0,$$

where $C^{0+\gamma}(D)$ represents the set of all functions that are Hölder continuous of degree $0 < \gamma < 1$.

Note that we frequently use the aforementioned notations and definitions, replacing D with $D^- \cup D^+$, $\bar{D}$, ∂D, $\partial D^{N,M}$,$\bar{D}^{N,\Delta t}$, and $\partial D^{N,\Delta t}$.

2 Statement of Continuous Problem

In this paper, we consider the following singularly perturbed parabolic convection-diffusion problems with the DIC defined on domain D:

$$\begin{cases} \mathcal{L}_\varepsilon u = u_t - \varepsilon u_{xx} + a(x,t)u_x + b(x,t)u = f(x,t), \quad (x,t) \in D, \\ u(x,0) = \phi(x), \quad 0 \le x \le 1; \quad [\phi](\tilde{d}) \ne 0, \quad 0 < \tilde{d} < 1; \\ u(0,t) = u(1,t) = 0, \quad 0 < t \le T; \end{cases} \tag{2.1}$$

where $D = \Omega \times (0,T], \Omega = (0,1), t \in (0,T], T > 0$, and $0 < \varepsilon \ll 1$ is a singular perturbation parameter and the coefficients $a(x,t), b(x,t)$ are smooth and satisfy $a(x,t) > \alpha > 0, \quad b(x,t) \ge \beta \ge 0 \quad$ on $\quad \bar{\Omega}$. We assume that the functions a, f, ϕ satisfy the below conditions:

$$a, f \in C^{4+\gamma}(D) \quad \text{for some} \quad \gamma > 0, \quad \text{and} \quad \phi^{(i)}(0) = 0 = \phi^{(i)}(1) = 0, \quad 0 \le i \le 4.$$

Moreover, $[\phi]$ denotes the jump in the function ϕ across the point of discontinuity $x = \tilde{d}$, that is, $[\phi](\tilde{d}) = \phi(\tilde{d^+}) - \phi(\tilde{d^-})$. In general, due to the presence of a discontinuity in the convection coefficient $a(x)$, the solution $u(x,t)$ of the problem (2.1) possesses an interior layer in the neighborhood of the point $x = \tilde{d}$. We observe that the initial function $\phi(x)$ is discontinuous at $x = \tilde{d}$ and the location of this point does not depend on the singular perturbation parameter ε. The initial condition ϕ is smooth, but it contains the interior layer in the vicinity of the layer $x = \tilde{d}$.

We assume that the initial data ϕ and f are sufficiently smooth functions on the domain $\bar{D}$ [28, 29] and that satisfy sufficient compatibility conditions at the corner points $(0,0)$ and $(1,0)$.

Assuming sufficient smoothness and compatibility conditions on ϕ and f, the parabolic problem (2.1) typically has a unique solution $u(x,t)$. This solution displays a regular boundary layer of width $O(\varepsilon)$ at $x = 1$. Additionally, in the range $a(t) > \alpha > 0, \quad 0 \le t \le T, \quad a, f \in C^{4+\gamma}(\bar{D})$, we presume that b and f constitute suitably regular layer components. Moreover, we assume adequate compatibility at the points $(0,0)$ and $(1,0)$ to ensure $u \in C^{4+\gamma}(\bar{D})$.

Let there be a point $\tilde{d} \in (0,1)$ such that ϕ is not continuous at $x = \tilde{d}$, but $\phi \in C^4(\bar{\Omega} \setminus \left\{\tilde{d}\right\})$.

Given $a > 0$, the function $\tilde{d}(t)$ exhibits monotonically increasing behavior. We assume that the convection term $a(x,t)$ is dependent on both the time and space and so the location of the interior layer does not remain at the same position throughout the process. Thus, we need to track the movement of the layer. The path of the characteristic curve Γ^* is defined by the following:

$$\Gamma^* = \left\{ \left(\tilde{d}(t), t\right) : \tilde{d}'(t) = a(\tilde{d}(t), t), \quad \tilde{d}(0) = \tilde{d}, \quad 0 < \tilde{d}(0) = \tilde{d} < 1 \right\} \tag{2.2}$$

We note that the characteristic curve Γ^* is generally not a straight line. Since $a(x,t) > 0$, the curve Γ is strictly increasing. Therefore, we have to restrict the final time T in order to avoid the overlap (to extend over or past

around and cover) between the interior layer and the boundary layer regions. We also restrict the size of the final time T so that the interior layer does not interact with the boundary layer. We note that Gracia and E. O'Riordan [8, 6] proved that the following relation can define the restriction: there exists some $\delta > 0$ such that

$$0 < \frac{1-\tilde{d}(T)}{1-\tilde{d}} = \delta < 1, \text{ where } \tilde{\mathrm{d}}\,(\mathrm{T}) \leq 1-\delta. \tag{2.3}$$

Next, we decompose the solution u of problem (2.1) into the following way:

$$u(x,t) = \frac{[\phi](\tilde{d})}{2} S(x-d,t) + y(x,t), \text{where}, \quad [\phi](\tilde{\mathrm{d}}) = \phi(\tilde{\mathrm{d}^+}) - \phi(\tilde{\mathrm{d}^-}) \tag{2.4}$$

The discontinuity in the initial condition generates an interior layer emanating from the point $(\tilde{d}, 0)$. By identifying the leading term $\frac{1}{2}[\phi](\tilde{d})\hat{\psi}_0$ in an asymptotic expansion of the solution, we can define the following continuous function

$$y(x,t) = u(x,t) - S(x,t) \tag{2.5}$$

where $S(x,t) = \frac{1}{2}[\phi](\tilde{d})\hat{\psi}_0(x,t)$, $\hat{\psi}_0(x,t) = erfc\left(\frac{\tilde{d}(t)-x}{2\sqrt{\varepsilon t}}\right)$, $erfc(z) = \frac{2}{\sqrt{\pi}}\int_{r=z}^{\infty} e^{-r^2} dr$ with

$$\mathcal{L}_\varepsilon y = f + \frac{1}{2}[\phi](\tilde{d})\left(a(\tilde{d}(t)-t) - a(x,t)\right)\frac{\partial}{\partial s}\hat{\psi}_0(x,t). \tag{2.6}$$

The function y satisfies the following problem:

$$\begin{cases} \mathcal{L}_\varepsilon y = 0, \quad (x,t) \in D, \\ y(0,t) = -\frac{1}{2}[\phi](\tilde{d})\hat{\psi}_0(0,t), \quad (0,T], \\ y(1,t) = -\frac{1}{2}[\phi](\tilde{d})\hat{\psi}_0(1,t) \quad (0,T], \quad y(x,0) = \begin{cases} \phi(x), & x < \tilde{d}, \\ \phi(\tilde{d}^-), & x = \tilde{d}, \\ \phi(x) - [\phi](\tilde{d}), & x > \tilde{d}. \end{cases} \end{cases} \tag{2.7}$$

2.1 Application of transformation to fix the location of interior layer

One possible choice for the transformation $X : (x,t) \to (v,t)$ is the piecewise linear map given by

$$v(x,t) = \begin{cases} \frac{\tilde{d}}{\tilde{d}(t)}x, & x \leq \tilde{d}(t), \\ 1 - \frac{1-\tilde{d}}{1-\tilde{d}(t)}(1-x), & x \geq \tilde{d}(t), \end{cases} \tag{2.8}$$

which means that $a(\tilde{d}(t),t) = a(\tilde{d},t)$. No transformation is needed if $a(x,t)$ is time-dependent only. We denote $a(v,t) = a(x,t)$ and $f(v,t) = f(x,t)$ as the transformed coefficient and source function in the v variable.
We also define two subdomains of D on either side of (left and right subdomains) Γ^* to be

$$D^- \to \Omega^- \times (0,T] = (0,\tilde{d}) \times (0,T] \quad and \quad D^+ \to \Omega^+ \times (0,T] = (\tilde{d},1) \times (0,T].$$

Applying this mapping for numerical solutions transforms (2.1) into the problem of finding y. Consequently, the transformed equation takes the form:

$$\begin{cases} \mathcal{L}_\varepsilon y = g\left(f + \frac{1}{2}[\phi](\tilde{d})\frac{\left(a(\tilde{d},t) - a(k,t)\right)}{\sqrt{\varepsilon\pi t}} e^{-\frac{g(k,t)(k-\tilde{d})^2}{4\varepsilon t}}\right), \quad x \neq \tilde{d} \\ [y]\,(\tilde{d},t) = 0, \quad \left[\frac{1}{\sqrt{g}}y_x\right](\tilde{d},t) = 0, \end{cases} \tag{2.9}$$

with the following transformed initial conditions,

$$y(p,t) = -\frac{1}{2}[\phi](\tilde{d})\hat{\psi}_0(p,t), \quad p \in \{0,1\}, \quad 0 \le t \le T, \tag{2.10}$$

$$y(x,0) = \begin{cases} \phi(x), & x < \tilde{d}, \\ \phi(\tilde{d}^-), & x = \tilde{d}, \\ \phi(x) - [\phi](\tilde{d}), & x > \tilde{d}. \end{cases} \tag{2.11}$$

Here, $\mathcal{L}_\varepsilon y = -\varepsilon y_{xx} + \kappa(x,t)y_x + g(x,t)y_t$, and the functions g, κ are defined by,

$$\kappa(x,t) = \sqrt{g}\left(a(x,t) + a(\tilde{d},t)(\hat{\psi}(x) - 1)\right),$$

$$g(x,t) = \begin{cases} \left(\frac{\tilde{d}(t)}{\tilde{d}}\right)^2, & x < \tilde{d}, \\ \left(\frac{1-\tilde{d}(t)}{1-\tilde{d}}\right)^2, & x > \tilde{d} \end{cases}, \quad \text{and} \quad \hat{\psi}(x) = \begin{cases} \frac{\tilde{d}-x}{\tilde{d}}, & x < \tilde{d}, \\ \frac{x-\tilde{d}}{1-\tilde{d}}, & x > \tilde{d}. \end{cases}$$

2.2 Decomposition of the solution

To develop sharp bounds in the error analysis, we decompose the solution $y(x,t)$ of (2.9) into the sum of smooth layer component $p(x,t)$, singular layer component $q(x,t)$ and the interior layer component $z(x,t)$ as follows:
$y(x,t) = p(x,t) + q(x,t) + \frac{1}{2}\sum_{i=2}^{4}[\phi^{(i)}](\tilde{d})\frac{(-1)^i}{i!}\hat{\psi}_i + z(x,t), \quad p,q \in C^{4+\gamma}(D).$
The smooth component $p(x,t)$ is represented using an asymptotic expansion:

$$p(x,t) = \sum_{i=0}^{3}\varepsilon^i p_i(x,t), \quad (x,t) \in \bar{D}.$$

where the functions $p(x,t)$ satisfy the following equations

$$\begin{cases} \partial\frac{\partial p_0}{\partial t} + a\frac{\partial p_0}{\partial x} + bp_0 = f, \quad \text{in} \quad D^- \cup D^+ \\ p_0(0,t) = u(0,t), \quad t \in (0,T], \quad p_0(x,0) = u(x,0), \quad x \in \bar{\Omega}, \\ \partial\frac{\partial p_1}{\partial t} + a\frac{\partial p_1}{\partial x} + bp_1 = -\frac{\partial^2 p_0}{\partial x^2}, \\ p_1(0,t) = 0, \quad p_1(1,t) = 0, \quad t \in (0,T], \quad p_1(x,0) = 0, \quad x \in \bar{\Omega} \\ \partial\frac{\partial p_2}{\partial t} + a\frac{\partial p_2}{\partial x} + bp_2 = -\frac{\partial^2 p_1}{\partial x^2}, \\ p_2(0,t) = 0, \quad t \in (0,T], \quad p_2(x,0) = 0, \quad x \in \bar{\Omega}, \end{cases} \tag{2.12}$$

and lastly, the functions p_3 satisfies

$$\begin{cases} \mathcal{L}_\varepsilon p_3 = -\frac{\partial^2 p_3}{\partial x^2}, \quad \text{in} \quad D \\ p_3(0,t) = p_3(1,t) = 0, \quad t \in (0,T], \quad p_3(x,0) = 0, \quad x \in \bar{\Omega}. \end{cases} \tag{2.13}$$

Hence, the smooth component of the solution satisfies the discontinuous function $p(x,t)$ by

$$\begin{cases} \mathcal{L}_\varepsilon p = f, \quad (x,t) \in D^- \cup D^+, \\ p(x,0) = y(x,0), \quad x \in \bar{\Omega}, \quad p(0,t) = y(0,t), \quad p(1,t) = y(1,t), \quad t \in (0,T]. \end{cases} \tag{2.14}$$

where $p(\tilde{d}^{\pm},t)=\lim_{x\to\tilde{d}\pm 0}p(x,t)$.

We define the discontinuous function $q(x,t)$, which represents the singular component of the decomposition, as follows:

$$\begin{cases} \mathcal{L}_\varepsilon q=0, \quad (x,t)\in D^-\cup D^+, \\ q(x,0)=0, \quad x\in\bar{\Omega} \\ q(0,t)=y(1,t)-p(0,t), \quad t\in(0,T]c \quad q(1,t)=y(1,t)-p^+(1,t), \quad t\in(0,T], \\ [q](\tilde{d},t)=-[p](\tilde{d},t), \quad \left[\frac{\partial q}{\partial x}\right](\tilde{d},t)=-\left[\frac{\partial p}{\partial x}\right](\tilde{d},t), \quad t\in(0,T] \end{cases} \tag{2.15}$$

Hence $q(\tilde{d}^-,t)=u(\tilde{d}^-,t)-p(\tilde{d}^-,t)$ and $q(\tilde{d}^+,t)=u(\tilde{d}^+,t)-p(\tilde{d}^+,t), \quad t\in(0,T]$.
The interior layer component $z(x,t)$ of the solution satisfies the discontinuous function by

$$\begin{cases} \mathcal{L}_\varepsilon z=f, \quad (x,t)\in D^-\cup D^+, \\ z(x,0)=0, \quad x\in\bar{\Omega}, \quad z(0,t)=0, \quad z(1,t)=0, \quad t\in(0,T]. \end{cases} \tag{2.16}$$

Note that, given the uniqueness of the solution to the problem (2.1), the decomposition $p+q+z$ remains valid.

Theorem 2.1. *The smooth component p defined in (2.14) belong to $C^{4+\gamma}(\bar{D}^{\pm})$ and the singular layer component q described in (2.15) belong to $C^{4+\gamma}(\bar{D}^{\pm})$ satisfy the following bounds for all non-negative integers i and m:*

$$\left\|\frac{\partial^{i+m}p}{\partial x^i\partial t^m}\right\|_{\bar{D}}\le C, \quad 0\le i+m\le 2, \quad ||\frac{\partial^3 p}{\partial x^3}||_{\bar{D}}\le C\varepsilon^{-1}, \quad x\neq\tilde{d},$$

and

$$\left\|\frac{\partial^{i+m}q}{\partial x^i\partial t^m}\right\|\le C\varepsilon^{-i}(1+\varepsilon^{2-j})e^{-\alpha(1-x)/\varepsilon}, \quad (x,t)\in D, \quad 0\le i+2m\le 4.$$

Then, when we combine these bounds with the bounds on the singular functions z, we get

$$y=p+q-\frac{1}{2}[\phi^{'}](\tilde{d})z_i(x,t), \quad p=p^+ +\frac{1}{2}\sum_{i=1}^{4}[\phi^i](\tilde{d})\frac{(-1)^i}{i!}z_i(x,t), \quad z_i\in C^{i-1+\gamma}(\bar{D}).$$

The interior layer function z_i is also bounded because p and q for $i=1,2,3,4$ are all constrained. **Proof**. The detailed proof is given in [10].

Theorem 2.2. *For any non-negative integers i,m, where $m\in\mathbb{N}\cup\{0\}$ satisfies $0\le i\le 3$ and $0\le i+2m\le 4$ in such a way that the smooth component p defined in (2.14) satisfy the following bounds:*

$$\left\|\frac{\partial^{i+m}p}{\partial x^i\partial t^m}(x,t)\right\|_{D^-\cup D^+}\le C, \quad 0\le i+2m\le 4$$

$$\left\|\frac{\partial^4 p}{\partial x^4}(x,t)\right\|\le C\varepsilon^{-1}, \quad (x,t)\in D^-\cup D^+,$$

and the boundary layer component q given in (2.15) satisfies the bounds

$$\left|\frac{\partial^{i+m}q}{\partial x^i\partial t^m}(x,t)\right|\le\begin{cases} C\left(\varepsilon^{-i}\exp(^{-(\tilde{d}-x)\alpha_1/\varepsilon})\right), & (x,t)\in D^-, \\ C\left(\varepsilon^{-i}\exp(^{-(x-\tilde{d})\alpha_2/\varepsilon})\right), & (x,t)\in D^+, \end{cases}$$

and

$$\left|\frac{\partial^4 q}{\partial x^4}(x,t)\right|\le\begin{cases} C\left(\varepsilon^{-4}\exp(^{-(\tilde{d}-x)\alpha_1/\varepsilon})\right), & (x,t)\in D^-, \\ C\left(\varepsilon^{-4}\exp(^{-(x-\tilde{d})\alpha_2/\varepsilon})\right), & (x,t)\in D^+. \end{cases}$$

where C is a constant independent of ε.

Proof. The detailed proof can be obtained by following the steps in Theorem 3.3 of [3].

3 Numerical Approximation

This section uses backward-Euler and central differences on a piecewise-uniform Shishkin mesh to approximate (2.7). We then discretize the singularly perturbed parabolic convection-diffusion problems with DIC (2.1) using backward-Euler for time and upwind finite differences for space, achieving ε-uniform convergence. The interior layer does not interact with the boundary layer at $x = 1$.

3.1 Construction of piecewise-uniform Shishkin mesh

Assuming that N and $M = \mathcal{O}(N)$ are both positive integers, we consider the domain $\bar{D} = \bar{\Omega} \times [0, T] = [0, 1] \times [0, T]$. We construct a piecewise uniform Shishkin mesh to handle the boundary layer at $x = 1$ in the singularly perturbed parabolic convection-diffusion problems with DIC (2.1). Given that the model problem displays boundary layers of width $\mathcal{O}(\sqrt{\varepsilon})$ and an interior layer starting at $x = \tilde{d}$, we define our rectangular mesh accordingly. We discretize the time derivative using the implicit Euler scheme on the mesh $\hat{\Omega}_t^M$. We establish the uniform temporal mesh as follows:

$$\hat{\Omega}_t^M = \{t_k : t_k = k\Delta t, \quad k = 0, \ldots, M, \quad t_0 = 0, \quad t_M = T, \quad \Delta t = T/M\},$$

where M is the number of mesh elements in the time direction, and step sizes k.
Let's denote the spatial mesh widths as $h_i = x_i - x_{i-1}$ and $\hat{h} = h_i + h_{i+1}$ for $i = 1, \ldots, N - 1$.
We divide the transformed spatial domain $\Omega = [0, 1]$ into the following four sub-intervals as follows

$$\bar{\Omega} = [0, \tilde{d} - \tau_1] \cup [\tilde{d} - \tau_1, \tilde{d}] \cup [\tilde{d} + \tau_2, 1 - \hat{\tau}_x] \cup [1 - \hat{\tau}_x, 1].$$

For the spatial mesh with N grids, the transition points τ_1, τ_2 and $\hat{\tau}_x$ are defined by

$$\begin{cases} \hat{\tau}_x = \min\left\{\dfrac{1}{4}, 2\sqrt{\varepsilon/\alpha}\ln N\right\}, \\ \tau_1 = \min\left\{\dfrac{\tilde{d} - \hat{\tau}_x}{4}, 2\sqrt{T\varepsilon}\ln N\right\}, \\ \tau_2 = \min\left\{1 - \tilde{d}(T), \dfrac{\tilde{d} - \hat{\tau}_x}{4}, 2\sqrt{T\varepsilon/\delta}\ln N\right\}. \end{cases} \tag{3.1}$$

The mesh interval point N of spatial grids are distributed into four intervals in the ratio $\dfrac{3N}{8} : \dfrac{N}{4} : \dfrac{N}{4} : \dfrac{N}{8}$ and each of them is spaced uniformly.
The spatial and temporal domains are denoted by $\hat{\Omega}_x^N$ and $\hat{\Omega}_t^M$ respectively. Thus, the discretized computational domain $\bar{D}^{N,M}$ is defined as

$$\bar{D}^{N,M} = \hat{\Omega}_x^N \times \hat{\Omega}_t^M, \quad \partial D^{N,M} = \bar{D}^{N,M} \setminus D^{N,M}.$$

where $\hat{\Omega}_x^N = \{x_i : x_{i-1} + h_i, x_0 = 0, x_N = 1, 1 \le i \le N\}$.
Then, obviously, $x_{N/2} = \tilde{d}$ and $\bar{\Omega}^N = \{x_i\}_{i=0}^N$. Further, let $h_1 = 2(1-\tau)/N$ and $h_2 = 2\tau/N$ be the mesh lengths in $[0, 1 - \tau]$ and $[1 - \tau, 1]$, respectively.

3.2 Numerical scheme in the transformed domain

3.2.1 The classical implicit upwind finite difference scheme

Before describing the computational scheme, for any discrete function $v_i^n \approx v(x_i, t_n)$, we define the first-order forward D_x^+, backward D_x^-, central D_x^0 difference operators, the backward finite difference operator D_t^- in time by

$$\begin{cases} D_x^+ Y(x_i, t_j) = \dfrac{Y(x_{i+1}, t_j) - Y(x_i, t_j)}{h_{i+1}}, \quad D_x^- Y(x_i, t_j) = \dfrac{Y(x_i, t_j) - Y(x_{i-1}, t_j)}{h_i}, \\ D_x^0 Y(x_i, t_j) = \dfrac{Y(x_{i+1}, t_j) - Y(x_{i-1}, t_j)}{h_i + h_{i+1}}, \quad \text{and} \quad D_t^- Y(x_i, t_j) = \dfrac{Y(x_i, t_j) - Y(x_i, t_{j-1})}{\Delta t}, \end{cases}$$

respectively, and define the second-order central finite difference operators δ_x^2 in space by

$$\delta_x^2 Y(x_i,t_j) = \frac{2}{h_i + h_{i+1}} \left(D_x^+ Y(x_i,t_j) - D_x^- Y(x_i,t_j) \right).$$

We discretize the transformed problem (2.9) and use the backward-Euler method for the time derivative and upwind finite difference scheme to approximate spatial derivatives. The discrete problem can be defined by the following: Find Y such that

$$\begin{cases} \mathcal{L}_\varepsilon^{N,M} Y^{N,\Delta t}(x_i,t_j) = f(x_i,t_j), \quad (x_i,t_i) \in D^{N,M} = \bar{D}^{N,M} \cap D, \\ \mathcal{L}_\varepsilon^{N,M} Y^{N,\Delta t}(x_i,t_j) = \left(D_t^- - \varepsilon \delta_x^2 + a D_x^- + bI \right) Y^{N,\Delta t}(x_i,t_j), \quad x_i \neq \tilde{d}, \quad t_j > 0, \\ \left[\frac{1}{\sqrt{g}} D_x^c Y \right] (\tilde{d},t_j) = 0, \quad x_i = \tilde{d}, t_j > 0, \\ Y_{ij} = y(x_i,t_j), \quad (x_i,t_j) \in \partial \bar{D}^{N,M}, \\ Y(0,t) = Y(1,t) = 0, \quad t_j \geq 0, \end{cases} \tag{3.2}$$

where

$$\left[\frac{1}{\sqrt{g}} D_x^c Y \right] (\tilde{d},t_j) = \frac{1-\tilde{d}}{(1-\tilde{d}(t_j))} D_x^+ Y(\tilde{d},t_j) - \frac{\tilde{d}}{\tilde{d}(t_j)} D_x^- Y(\tilde{d},t_j).$$

The upwind finite difference operator corresponds to this discrete problem: Define for any mesh function U:

$$\begin{cases} \left(D_t^- - \varepsilon \delta_x^2 + a D_x^- + bI \right) U^{N,\Delta t}(x_i,t_j) = f(x_i,t_j), \quad x_i \neq \tilde{d}, \quad t_j > 0, \\ -\varepsilon \left[\frac{1}{\sqrt{g}} D_x^c U \right] (\tilde{d},t_j) = 0, \quad x_i = \tilde{d}, \quad t_j > 0, \\ U(x_i,t_j) = u(x_i,t_j), \quad (x_i,t_j) \in \partial D^{N,\Delta t}, \end{cases} \tag{3.3}$$

where

$$\left[\frac{1}{\sqrt{g}} D_x^c U \right] (\tilde{d},t_j) = \frac{1-\tilde{d}}{(1-\tilde{d}(t_j))} D_x^+ U(\tilde{d},t_j) - \frac{\tilde{d}}{\tilde{d}(t_j)} D_x^- U(\tilde{d},t_j),$$

At the (x_i,t_j) node of the mesh, the numerical approximation of the PDE is written as

$$-\varepsilon \delta_x^2 Y_{ij} + a_j D_x^- Y_{ij} + b_j U_{ij} + D_t^- Y_{ij} = f_{ij}.$$

Upon substituting the definition of the finite difference scheme and rearranging the term one may obtain

$$-A_i Y_{i+1,j} + B_{ij} Y_{ij} - C_{ij} Y_{i-1,j} - D Y_{i,j-1} = f_{ij}$$

where the coefficients in the upwind finite difference scheme are given by

$$\begin{cases} A_i = \left(\dfrac{-2\varepsilon}{h_{i+1}(h_i + h_{i+1})} \right), \\ B_{ij} = \left(\dfrac{2\varepsilon}{h_{i+1}(h_i)} + \dfrac{a_j}{h_i} + b_j + \dfrac{1}{\Delta t} \right), \\ C_{ij} = \left(\dfrac{2\varepsilon}{h_{i+1}(h_i + h_{i+1})} + \dfrac{a_j}{h_i} \right), \\ D = \dfrac{1}{\Delta t}. \end{cases} \tag{3.4}$$

Here, $\Delta t = t_j - t_{j-1}$, $\quad a_j = a(t_j)$, $\quad b_j = b(t_j)$ and

$$Y_{i0} = Y(x_i,t_0) = y(0,t_j), \quad Y_{0j} = Y(x_0,t_j) = y(0,t_j), \quad Y_{Nj} = Y(x_N,t_j) = y(1,t_j).$$

The above numerical equation is converted into a matrix equation of the form $\Lambda \overrightarrow{Y} = \overrightarrow{C}$, where Λ is the coefficient of the matrix and $\overrightarrow{C}$ is the constant vector.

The global approximation $\bar{Y}$ is done using simple bilinear interpolation:

$$\bar{Y}(x,t) = \sum_{i=0,j=1}^{N,M} Y_{ij}\varphi_i(x)\eta_j(t)$$

where $\mu_i(x)$ is the standard hat function centered at $x = x_i$ and is defined by

$$\varphi_i(x) = \begin{cases} \dfrac{x - x_{i-1}}{h_i}, & \text{if} \quad x_{i-1} \le x \le x_i, \\ \dfrac{x_{i+1} - x}{h_{i+1}}, & \text{if} \quad x_i \le x \le x_{i+1} \\ 0, \quad otherwise. \end{cases} \tag{3.5}$$

and

$$\eta_j(t) = \begin{cases} \dfrac{t - t_{j-1}}{\Delta t}, & \text{if} \quad t_{j-1} \le t \le t_j, \\ 0, \quad otherwise. \end{cases} \tag{3.6}$$

Once $\bar{Y}$ is found, $\bar{U}$ can easily be computed as $\bar{U} = \bar{Y} + S$.

One can demonstrate that the finite difference operator $\mathcal{L}_\varepsilon^{N,M}$ obeys the well-known discrete minimum principle, resulting in ε-uniform stability of the difference operator $\mathcal{L}_\varepsilon^{N,M}$.

Lemma 3.1. *(Discrete Minimum Principle)*
Suppose Θ be any mesh function defined on $\bar{D}^{N,M}$. If $\Theta(x_i,t_n) \le 0$ on $\Gamma^{N,M} = \bar{D}^{N,M} \cap \Gamma$ and $\mathcal{L}_\varepsilon^{N,M}\Theta(x_i,t_n) \le 0$ in $D^{N,M}$, then $\Theta(x_i,t_n) \ge 0$ in $\bar{D}^{N,M}$.

Proof. The detailed proof is given in [13].
The following theorem affirms that the error estimate for the numerical scheme given in equations (3.2) demonstrates ε-uniform convergence when applied on the generated piecewise-uniform (Shishkin) mesh with almost first-order accuracy.

Theorem 3.2. *For large enough N and $M = \mathcal{O}(N)$. If Y is the solution of the discrete problem (3.2) and y is the solution of (2.9), then the global approximation of $\bar{Y}$ on $\bar{D}^{N,M}$ and bilinear interpolation and the error associated with the discrete solution $Y^{N,\Delta t}$ at time level t_n is given by satisfies:*

$$\left| y(x_i,t_n) - \bar{Y}^{N,\Delta t}(x_i,t_n) \right| \le C\left(N^{-1}\ln N + \Delta t\right), \quad (x_i,t_n) \in D^{N,M}, \quad 1 \le i \le N-1. \tag{3.7}$$

Proof The detailed proof is given in [30, 24].

Theorem 3.3. *Suppose u is the collection of the problem (2.1) in the transformed domain and $U^{N,M}$ be the solution of the discrete problem (3.3) on the Shishkin mesh $\bar{D}^{N,M}$. If $\hat{U}$ is the solution obtained from U using the Richardson extrapolation technique, then the global error satisfies the following estimates*

$$||\hat{U}(x_i,t_n) - u(x_i,t_n)|| \le C\left(N^{-2}\ln^2 N + M^{-2}\right), \quad (x_i,t_n) \in D^{N,M}, \quad 1 \le i \le N-1. \tag{3.8}$$

Proof The detailed proof can be found in n [30, 24].

This article aims to enhance the discrete solution $Y^{N,\Delta t}$ of the problem (2.1) through post-processing. Our objective is to achieve a uniform order of accuracy greater than one in both spatial and temporal variables for the singularly perturbed parabolic convection-diffusion problems(2.1) using the Richardson extrapolation technique.

4 Richardson Extrapolation of $Y^{N,\Delta t}$ in the Transformed Domain

This paper aims to enhance the accuracy of the upwind scheme (3.2) in the transformed domain using Richardson extrapolation. The numerical solution is denoted as $Y^{N,M}$ on the mesh $D^{N,M}$. To increase convergence, we use technique (3.2) on a finer mesh $\bar{D}^{2N,2M} = \bar{\Omega}_x^{2N} \times \bar{\Omega}_x^{2M}$ with $2N$ mesh intervals in the spatial directions and $2M$ in the t-direction intervals, with a piecewise-uniform Shishkin mesh $\bar{\Omega}_x^{2N}$ having the same transition point $1-\tau$ shared with $\bar{\Omega}_x^N$. This mesh is created by bisecting intervals of $\bar{\Omega}_x^N$

Clearly, $\bar{D}_x^{N,M} = \{(x_i, t_n)\} \subset \bar{D}_x^{2N,2M} = \{(\hat{x}_i, \hat{t}_n)\}$. Thus, on $\bar{D}^{2N,2M}$, one has $\hat{x}_i - \hat{x}_{i-1} = h/2$ for $\hat{x}_i \in [0, 1-\tau]$ and $\hat{x}_i - \hat{x}_{i-1} = H/2$ for $\hat{x}_i \in [1-\tau, 1]$.

Let $\hat{Y}^{2N,\Delta t/2}$ represent the solution of the discrete problem (3.2) on the mesh $\bar{\Omega}^{2N,2M}$. Therefore, it follows from the Theorem 3.2, we can express the error as follows:

$$Y^{N,\Delta t}(x_i, t_n - y(x_i, t_n) = C\left(N^{-1}\ln N + \Delta t\right) + R^{N,\Delta t}(x_i, t_n), \tag{4.1}$$

$$= C\left(N^{-1}\left(2\sqrt{T\varepsilon}\ln N\right) + \Delta t\right) + R^{N,\Delta t}(x_i, t_n), \quad (x_i, t_n) \in \bar{D}^{N,M}, \tag{4.2}$$

where C is a fixed constant and the remainder term $R^{N,\Delta t}$ is $o(N^{-1}\ln N + \Delta t)$.

Given that $\hat{Y}^{2N,\Delta t/2}$ is derived using the same transition point $1-\tau$, we have

$$\hat{Y}^{2N,\Delta t/2}(x_i, t_n) - y(x_i, t_n) = C\left((2N)^{-1}\left(2\sqrt{T\varepsilon}\ln N\right) + (\Delta t/2)\right) + R^{2N,\Delta t/2}(\hat{x}_i, \hat{t}_n), (\hat{x}_i, \hat{t}_n) \in \bar{D}^{2N,2M}, \tag{4.3}$$

where the remainder term $R^{2N,\Delta t/2}$ is $o(N^{-1}\ln N + \Delta t)$.

Multiplying equation (4.3) by 2 and subtracting it from equation (4.2), we eliminate first order term $O(N^{-1})$ and $O(\Delta t)$, resulting in the following approximation, from which we can derive:

$$y(x_i, t_n) - \left(2\hat{Y}^{2N,\Delta t/2}(x_i, t_n) - Y^{N,\Delta t}(x_i, t_n)\right) = R^{2N,\Delta t/2}(\hat{x}_i, \hat{t}_n) - R^{N,\Delta t}(x_i, t_n), \quad (x_i, t_n) \in \bar{D}^{N,M},$$

$$= o\left(N^{-1}\ln N + \Delta t\right), \quad (x_i, t_n) \in \bar{D}^{N,M}.$$

Therefore, we shall use the following extrapolation formula

$$Y_{extp}^{N,\Delta t}(x_i, t_n) = 2\hat{Y}^{2N,\Delta t/2}(x_i, t_n) - Y^{N,\Delta t}(x_i, t_n), \quad (x_i, t_n) \in \bar{D}^{N,M}. \tag{4.4}$$

the numerical solution becomes more accurate than both $\hat{Y}^{2N,\Delta t/2}(x_i, t_n)$ and $Y^{N,\Delta t}(x_i, t_n)$ to approximate the exact solution of the given model problem (2.1).

The truncation error of the spatial discretization in the approximation of (4.4) becomes

$$\left|y(x_i, t_n) - \hat{Y}_{extp}^{N,\Delta t}(x_i, t_n)\right| \leq C(N^{-2} + \Delta t^2). \tag{4.5}$$

4.1 Decomposition of discrete solutions in the transformed domain

Similar to the continuous solution, we decompose the discrete solution $Y^{N,M}(x_i, t_j)$ into the regular $P(x_i, t_j)$, singular $Q(x_i, t_j)$ and $Z(x_i, t_i)$ is the interior layer. We will estimate the nodal error $\left|Y^{N,M}(x_i, t_j) - y(x_i, t_j)\right|$ by decomposing the solution $Y^{N,M}(x_i, t_j)$ on the mesh $D^{N,M}$ in the following manner:

$$\underbrace{Y}_{\text{Numerical solution}} = \underbrace{P}_{\text{Smooth solution}} + \underbrace{Q}_{\text{Boundary component}} + \underbrace{Z}_{\text{Interior component}}$$

Here, P, Q, and Z represent the discrete counterparts of the continuous components p, q, and z, respectively. Define P_L and P_R as the solutions to the respective discrete problems, approximating p to the left and right of the discontinuity at $x = \tilde{d}$:

$$\begin{cases} \mathcal{L}_{\varepsilon}^{N,M} P_L = f\left(x_i, t_j\right), \quad (x_i, t_j) \in D^N \cap \bar{D}^-, \\ P_L(0, t_j) = y(0, t_j), \quad P_L(\tilde{d}, t_j) = p(\tilde{d}^-, t_j), \quad t_j > 0, \\ P_L(x_i, 0) = p(x_i, 0), \quad x_i \leq \tilde{d}, \end{cases} \tag{4.6}$$

and

$$\begin{cases} \mathcal{L}_{\varepsilon}^{N,M} P_R = f\left(x_i, t_j\right), \quad (x_i, t_j) \in D^N \cap \bar{D}^-, \\ P_R(1, t_j) = y(1, t_j), \quad P_R(\tilde{d}, t_j) = p(\tilde{d}^+, t_j), \quad t_j > 0, \\ P_R(x_i, 0) = p(x_i, 0), \quad x_i \geq \tilde{d}, \end{cases} \tag{4.7}$$

Similarly, for the solutions of the following discrete problems, we define the mesh functions $Q_L : \bar{D}^N \cap [0, \tilde{d}] \to R$ and $Q_R : \bar{D}^N \cap [\tilde{d}, 1] \to R$ (which are approximate q to the left and right of the discontinuity $x = \tilde{d}$).

$$\begin{cases} \mathcal{L}_{\varepsilon}^{N,M} Q_L = 0, \quad (x_i, t_j) \in D^N \cap \bar{D}^-, \\ \mathcal{L}_{\varepsilon}^{N,M} Q_R = 0, \quad (x_i, t_j) \in \bar{D}^N \cap \bar{D}^+, \\ Q_L(0, t_j) = 0, \quad Q_L(x_i, 0) = 0, \quad x_i \leq 0, \\ Q_R(x_i, 0) = 0, \quad x_i \geq \tilde{d}, \quad Q_R(1, t_j) = 0, \\ Q_R(\tilde{d}, t_j) + P_R(\tilde{d}, t_j) = Q_L(\tilde{d}, t_j) + P_L(\tilde{d}, t_j), \\ D_x^+ Q_R(\tilde{d}, t_j) + D_x^+ P_R(\tilde{d}, t_j) = D_x^- Q_L(\tilde{d}, t_j) + D_x^- P_L(\tilde{d}, t_j). \end{cases} \tag{4.8}$$

Finally, we can define the discrete solution U as

$$U(x_i, t_j) = \begin{cases} P_L(x_i, t_j) + Q_L(x_i, t_j), \quad (x_i, t_j) \in D^N \cap \bar{D}^-, \\ P_L(\tilde{d}, t_j) + Q_L(\tilde{d}, t_j) = P_R(\tilde{d}, t_j) + Q_L(\tilde{d}, t_j), \quad x_i = \tilde{d}, \\ Q_R(x_i, t_j) + P_R(x_i, t_j), \quad (x_i, t_j) \in \bar{D}^N \cap \bar{D}^+. \end{cases} \tag{4.9}$$

4.2 Error Analysis

In this section, we establish error bounds for the extrapolated discrete solution from (3.2) corresponding to the problem (2.1). Instead of directly assessing the nodal error of $(U_{extp}^{N,M})$, we will individually analyze the nodal errors of its smooth component $(P_{extp}^{N,M})$ and its singular component $(Q_{extp}^{N,M})$. These outcomes will be amalgamated to formulate a uniform error estimate concerning ε-uniformity for the extrapolated solution in (4.4).

4.2.1 Error estimate for the smooth component P

Lemma 4.1. *Given $\varepsilon \leq N^{-1}$, the local truncation error for the smooth component is bounded by:*

$$\mathcal{L}_{\varepsilon}^{N,M}(P - p)(x_i, t_{n+1}) = h_1 \xi_1(x_i, t_{n+1}) + \Delta t \xi_2(x_i, t_{n+1}) + O(H^2), \quad \textit{for} \quad 1 \leq i \leq N - 1,$$

where

$$\xi_1(x, t) = \frac{1}{2} a(x, t) \frac{\partial^2 p}{\partial x^2}(x, t), \quad \text{and} \quad \xi_2(x, t) = \frac{1}{2} \frac{\partial^2 p}{\partial x^2}(x, t), \quad (x, t) \in D.$$

Proof. It is easy to obtain the local truncation error associated with the smooth component $P^{\pm}$:

$$\mathcal{L}_{\varepsilon}^{N,M}(P - p)(x_i.t_{n+1}) = -\frac{\varepsilon}{3\hat{h}_i} \left[h_{i+1}^2 \frac{\partial^3 p}{\partial x^3}(\chi_1, t_{n+1}) - h_i^2 \frac{\partial^3 p}{\partial x^3}(\chi_2, t_{n+1}) \right] - \frac{h_{i+1}}{2} a(x_i) \frac{\partial^2 p}{\partial x^2}(x_i, t_{n+1}) -$$

$$\frac{h_{i+1}^2}{3!}a(x_i)\frac{\partial^3 p}{\partial t^3}(\chi_3,t_{n+1})-\frac{\Delta t}{2}\frac{\partial^3 p}{\partial x^3}(x_i,t_{n+1})+\frac{\Delta t^2}{3!}\frac{\partial^3 p}{\partial t^3}(x_i,\sigma),$$

for some $\chi_1, \quad \chi_3 \in (x_i, x_{i+1}), \quad \chi_2 \in (x_{i-1}, x_i)$ and $\sigma \in (t_n, t_{n+1})$.
Following Keller's approach [31], we define the functions $\tilde{E}_k, \quad k = 1, 2$, which satisfies the following problems:

$$\begin{cases} \mathcal{L}_\varepsilon \tilde{E}_k = \phi_k, \quad in \quad D, \\ \tilde{E}_k(x,0) = \quad x \in \bar{\Omega}, \quad \tilde{E}_k(0,t) = \tilde{E}_k(1,t) = 0, \quad t \in (0,T]. \end{cases} \tag{4.10}$$

Hence, $\tilde{E}_k$ decomposes as $\tilde{E}_k = \psi_k + \mu_k, \quad k = 1, 2,$, where the smooth component ψ_k and the boundary component μ_k satisfy the following IBVPs

$$\begin{cases} \mathcal{L}_\varepsilon \psi_k = \Phi_k, \quad \mathcal{L}\mu_k = 0, \quad \text{in} D, \\ \psi_k(x,0) = \mu_k(x,0) = 0, \quad x \in \bar{\Omega}, \\ \psi_k(0,t) = \mu_k(0,t) = 0, \\ \psi_k(1,t) = -\mu_k(1,t), \quad t \in (0,T], \quad k = 1, 2. \end{cases} \tag{4.11}$$

Theorem 4.2. *The smooth components $\psi_k, \quad k = 1, 2$ defined in (4.11) satisfy the following bounds*

$$\left\| \frac{\partial^{i+m}\psi_k}{\partial x^i \partial t^m} \right\|_D \leq C, \quad \left\| \frac{\partial^3 v}{\partial x^3}(x,t) \right\| \leq C\varepsilon^{-1},$$

where for all non-negative integers $i, m, \quad 0 \leq i + m \leq 2$.
Proof. The detailed proof is given in [13, 32].

Lemma 4.3. *Assume that $\varepsilon \leq N^{-1}$. Then, we have*

$$\begin{cases} |(P_L - p)(x_i, t_n)| \leq C\left(N^{-2} + \Delta t^2\right), \quad for \quad 1 \leq i \leq N/2 - 1, \\ |(P_R - p)(x_i, t_n)| \leq C\left(N^{-2} + \Delta t^2\right), \quad for \quad N/2 + 1 \leq i \leq N - 1. \end{cases} \tag{4.12}$$

Proof: The poof of detail is given by y [13, 28, 32].

Lemma 4.4. *Assume that $\varepsilon \leq N^{-1}$. Then, we have*

$$(P - p)(x_i, t_{n+1}) = h_i\psi_1(x_i, t_{n+1}) + \Delta t\psi_2(x_i, t_{n+1}) + O\left(N^{-2} + \Delta t^2\right), \quad 1 \leq i \leq N - 1.$$

Proof. The detailed proof is given in in [13, 32].

Lemma 4.5. *Assume that $\varepsilon \leq N^{-1}$, the extrapolation error for the smooth component P is bounded by:*

$$\left| p(x_i, t_{n+1}) - P_{extp}^{N,\Delta t}(x_i, t_{n+1}) \right| (x_i, t_{n+1}) = O\left(N^{-2} + \Delta t^2\right), \quad for \quad 1 \leq i \leq N - 1.$$

Proof. Given that the mesh widths of $\bar{D}^{2N,2M}$ are half that of $\bar{D}^{N,M}$, applying Lemma 4.4 on the finest mesh $D^{2\bar{N},2m}$, we obtain:

$$\left(\tilde{P}^{2N,\Delta t} - p\right)(x_i, t_{n+1}) = \begin{cases} (H/2)\psi_1(x_i, t_{n+1}) + (\Delta t/2)\psi_2(x_i, t_{n+1}) + O\left(N^{-2} + \Delta t^2\right), \quad 1 \leq i \leq N/2, \\ (h/2)\psi_1(x_i, t_{n+1}) + (\Delta t/2)\psi_2(x_i, t_{n+1}) + O\left(N^{-2} + \Delta t^2\right), \quad N/2 + 1 \leq i \leq N - 1. \end{cases} \tag{4.13}$$

Therefore, according to the extrapolation formula (4.4), Lemma 2.1, and (4.13) it immediately follows that

$$\begin{aligned} p(x_i, t_{n+1}) - P_{extp}^{N,\Delta t}(x_i, t_{n+1}) &= p(x_i, t_{n+1}) - \left(\tilde{P}^{2N,\Delta t}(x_i, t_{n+1}) - P^{N,\Delta t}(x_i, t_{n+1})\right) \\ &= 2\left(\tilde{P}^{N,\Delta t} - p(x_i, t_{n+1})\right) + \left(P^{N,\Delta t} - p\right)(x_i, t_{n+1}) \\ &= O\left(N^{-2} + \Delta t^2\right), \quad \text{for} \quad 1 \leq i \leq N - 1. \end{aligned}$$

4.2.2 Error estimate for the singular layer component Q

Prior to the extrapolation analysis, we introduce a crucial lemma for the subsequent section. We define the piecewise $(0,1)$-Padé approximation of $\exp\left(\frac{-\alpha x_i}{\varepsilon}\right)$ on the mesh Ω_1^N, where $i = 0, 1, \ldots, N$, as the following mesh functions:

$$S_i = \prod_{k=1}^{i} \left(1 + \frac{\alpha h_k}{\varepsilon}\right), \quad S_i^{'} = \prod_{k=1}^{i} \left(1 + \frac{\alpha h_k}{2\varepsilon}\right)$$

then $S_i \geq \exp(\frac{-\alpha x_i}{\varepsilon})$,where by convection $S_0 = S_0^{'} = 1$.

Lemma 4.6. *On the domain $\bar{\Omega}^N = \bar{\Omega}_x^{N,\varepsilon}$, define the following two mesh functions*

$$S_i = \prod_{k=1}^{i} \left(1 + \frac{\gamma h_j}{\varepsilon}\right), \quad \textit{for} \quad 1 \leq i \leq N/2, \tag{4.14}$$

$$M_i = \prod_{k=1}^{i} \left(1 + \frac{\gamma \bar{h}_j}{\varepsilon}\right), \quad \textit{for} \quad N/2 \leq i \leq N-1, \tag{4.15}$$

(Using the usual convention that if $i = 0$, then $S_0 = 1$ and if $i = N$, then $M_N = 1$), where γ is a positive constant.

Lemma 4.7. *The following inequalities hold true:*

$$\exp\left(-\gamma(\tilde{d} - x_i)/\varepsilon\right) \leq \prod_{N/2}^{j=i+1} \left(1 + \frac{\gamma h_j}{\varepsilon}\right)^{-1}, \quad \textit{for} \quad 1 \leq i \leq N/2 - 1, \tag{4.16}$$

and

$$\exp\left(-\gamma(x_i - \tilde{d})/\varepsilon\right) \leq \prod_{j=N-i+1}^{N/2} \left(1 + \frac{\gamma \bar{h}_j}{\varepsilon}\right)^{-1}, \quad \textit{for} \quad N/2 \leq i \leq N-1. \tag{4.17}$$

Proof. For each j, we have

$$\exp(-\gamma h_j/\varepsilon) = (\exp(\gamma h_j/\varepsilon))^{-1} \leq (1 + \frac{\gamma h_j}{\varepsilon})^{-1}; \tag{4.18}$$

and similarly,

$$\exp(-\gamma \bar{h}_j/\varepsilon) \leq (1 + \frac{\gamma \bar{h}_j}{\varepsilon})^{-1}. \tag{4.19}$$

Hereby, we deduce the result (4.16) by multiplying the inequalities obtained from (4.18), for $j = i+1, \ldots N/2$ and the result (4.17) follows from multiplication of (4.19), for $j = N - i + 1, \ldots, N/2$.

Lemma 4.8. *The error associated with the singular component of the boundary layer satisfies Q*

$$|q(x_i, t_{n+1}) - Q_{extp}(x_i, t_{n+1})| \leq CN^{-2}, \quad \textit{for} \quad 1 \leq i \leq N/2.$$

Proof. The detailed proof is given in [13, 22].

Lemma 4.9. *For $N/2 + 1 \leq i \leq N - 1$, the local truncation associated with the boundary layer component satisfies*

$$\mathcal{L}_\varepsilon \left(Q - q\right)(x_i, t_{n+1}) \leq \begin{cases} \left(N^{-1} \ln N\right) \zeta_1(x_i, t_{n+1}) + \Delta t \zeta_2 \mathcal{O}\left(\varepsilon^{-1}\right) \exp^{-\alpha(1-x_{i+1})/\varepsilon} N^{-2} \ln^2 N + \exp^{(-\alpha(1-x_i)/\varepsilon)}, \\ \left(N^{-1} \ln N\right) \zeta_1(x_i, t_{n+1}) + \Delta t \zeta_2 \mathcal{O}\left(\varepsilon^{-1}\right) \exp^{-\alpha(1-x_{i+1})/\varepsilon} N^{-2} \ln^2 N + \exp^{(-\alpha(1-x_i)/\varepsilon)}. \end{cases}$$

Proof. One can refer to the detailed proof given in [33].

Lemma 4.10. *The error after extrapolation associated to the layer component $Q^{N,\Delta t}$ satisfies*

$$|q(x_i,t_{n+1}) - Q_{extp}(x_i,t_{n+1})| \le C\left(N^{-2}\ln^2 N + \Delta t^2\right), \quad \textit{for} \quad N/2+1 \le i \le N-1.$$

Proof.The poof of detail is given by en by [13].
The following theorem presents the key result of this section, summarizing the error estimates after extrapolation.

Theorem 4.11. *(Overall error after extrapolation) The solution y of (2.1) and its discrete counterpart Y for (3.2) meet the following error estimate:*

$$|y(x_i,t_n) - Y^{N,M}_{extp}(x_i,t_n)| \le C\left(N^{-2}\ln^2 N + \Delta t^2\right), \quad 1 \le i \le N-1. \tag{4.20}$$

Proof. Hence, equation (4.20) directly follows from the combination of Lemma 4.5 applied to the smooth component, and Lemma 4.10 for the layer component.

5 Numerical Examples, Results and Discussion

In this section, we validate theoretical results by applying the Richardson extrapolation method alongside a classical upwind scheme to a test problem. We conduct numerical tests to affirm theoretical findings, employing model problems from equations (2.1) and utilizing the numerical scheme outlined in equations (3.2). This section showcases three examples. Given that exact solutions are unknown, we evaluate the maximum point-wise error utilizing the double mesh principle ciple [9,6].
Let $\bar{Y}^{N,M}$ denote the bilinear interpolation of the discrete solution $Y^{N,M}$ on the piecewise-uniform Shishkin mesh $\bar{D}^{N,M}$. Then, the maximum point-wise of the double mesh principle of global difference is given by

$$E^{N,M}_{\varepsilon} = ||\bar{Y}^{N,M}(x_i,t_n) - \bar{Y}^{2N,2M}(x_i,t_n)||.$$

For each ε the corresponding order of convergence $P^{N,M}$ is computed as

$$P^{N,M} = \log_2\left(\frac{E^{N,M}_{\varepsilon}}{E^{2N,2M}_{\varepsilon}}\right).$$

Also, the ε-uniform maximum point-wise error $E^{N,M}$ and the corresponding ε-uniform order of convergence $P^{N,M}$ is given by

$$E^{N,M} = \max_{\varepsilon} E^{N,M}_{\varepsilon}, \quad P^{N,M} = \log_2\left(\frac{E^{N,M}_{\varepsilon}}{E^{2N,2M}_{\varepsilon}}\right) \quad \text{and} \quad P^{N,M}_{\text{extp}} = \log 2\left(\frac{E^{N,M}_{\varepsilon,extp}}{E^{2N,2M}_{\varepsilon,extp}}\right).$$

For each value of N satisfying $N, 2N \in R_N = [32, 64, 128, 256, 512, 1024, 2048]$, we calculate the ε-uniform maximum pointwise double-mesh differences $E^{N,M}$.

In our experiments, we examine the parameter set $\varepsilon = \{2^0, \ldots, 2^{-18}\}$. We calculate solutions $Y^{N,M}$ and $Y^{2N,2M}$ using (3.2) on piecewise-uniform Shishkin meshes $\bar{E}^{N,M}$ and $\bar{E}^{2N,2M}$ with $N = M = 64$. For all three test examples, we provide plots of $\bar{Y}^{N,M}$ and $\bar{U}^{N,M} = \bar{Y}^{N,M} + \bar{S}$ for $\varepsilon = 2^{-12}$ and $N = M = 64$.

The interior layers do not interact with the boundary layer in the first two examples and in the third example, the interior layer does interact with the boundary layers.

5.1 Classical upwind finite difference scheme

Example 5.1. *Consider the following singularly perturbed parabolic problem:*

$$\begin{cases} -\varepsilon u_{xx} + x(1+t^2)u_x + u_t = 4x\,(1-x)\,t + t^2, & (x,t) \in (0,1)\times(0,1/2], \\ u(0,t) = -2, \quad u(1,t) = 1, & 0 < t \le 0.5. \end{cases} \tag{5.1}$$

The discontinuous initial condition is given by

$$u(x,0) = \phi(x) = \begin{cases} -2; & 0 \le x < \tilde{d}, \\ 1; & \tilde{d} \le x \le 1. \end{cases} \tag{5.2}$$

where $\tilde{d} = 0.3, \quad T = 0.5$ and $\alpha = 1$.
The corresponding continuous function is given by

$$y(x,t) = u(x,t) - S(x,t), \quad S = \frac{1}{2}[\phi^{'}](\tilde{d})e^{B(t)}\psi_0(x,t)$$

with $[\phi](\tilde{d}) = \lim_{x\to\tilde{d}^+}\phi(x) - \lim_{x\to\tilde{d}^-}\phi(x) = \phi(\tilde{d}^+) - \phi(\tilde{d}^-) = 1 - (-2) = 3$,
$B(t) = \int_0^t b(t^{'})dt^{'} = 0$ and $\psi_0(x,t) = erf(z)$. $z = \dfrac{\tilde{d}(t) - x}{2\sqrt{\varepsilon t}}, \quad erfc(z) = \dfrac{2}{\pi}\displaystyle\int_z^\infty e^{-s^2}ds.$
The characteristics curve $\Gamma^* : \tilde{d}(t) = \tilde{d} + \int_0^t a(t^{'})dt^{'} = 0.3 + t + t^3/3$.

Example 5.2. *Consider the following singularly perturbed parabolic problem:*

$$\begin{cases} u_t - \varepsilon u_{xx} + x(1+t)u_x = 4x\,(1-x)\,t + t^2, & (x,t) \in (0,1)\times(0,1/2], \\ u(0,t) = u(1,t) = 0, \quad 0 < t \le 0.5. \end{cases} \tag{5.3}$$

The discontinuous initial condition is given by

$$u(x,0) = \phi(x) = \begin{cases} -x^3; & 0 \le x < \tilde{d}, \\ (1-x)^3; & \tilde{d} \le x \le 1, \end{cases} \tag{5.4}$$

where $\tilde{d} = 0.3, \quad T = 0.5, \quad \alpha = 1$.

Example 5.3. *Consider the following singularly perturbed parabolic problem:*

$$\begin{cases} u_t - \varepsilon u_{xx} + x(1+t)u_x = 4x\,(1-x)\,t + t^2, & (x,t) \in (0,1)\times(0,1/2], \\ u(0,t) = -2, \quad u(1,t) = 1, \quad 0 < t \le 0.5, \end{cases} \tag{5.5}$$

where $\tilde{d} = 0.3, \quad T = 2, \quad \alpha = 1$ and $[\phi^{'}](0.3) = 0$ and the characteristics curve $\Gamma^* : \tilde{d}(t) = t + t^2/2 + 0.3$.
The discontinuous initial condition is given by

$$u(x,0) = \phi(x) = \begin{cases} -2; & 0 \le x < \tilde{d}, \\ 1; & \tilde{d} \le x \le 1. \end{cases} \tag{5.6}$$

In this example, the final time has been selected to be sufficiently large, so that the interior layer interacts with the boundary layer.

In the first and second examples, the interior layer does not interact with the boundary layer. But, in the third example, the interior layer interacts with the boundary layer.

Fig. 1, 2, and 3 shows computed approximations for Y and the numerical solution U with the scheme (3.2) and presents a surface plot of the numerical solution with $N = M = 64$ and $\varepsilon = 2^{-12}$. Unlike Example 1, where $[\phi^{'}](0.3) \neq 0$, here the influence of the initial condition on the convergence order is apparent. The order is reduced to 0.5, aligning with the error bound from Theorem 3.2. Tables display uniform double mesh global differences, demonstrating almost first-order convergence when approximating component $\tilde{d}$. The results presented in the tables provide support for the theoretical error estimates outlined in Theorem 3.2.

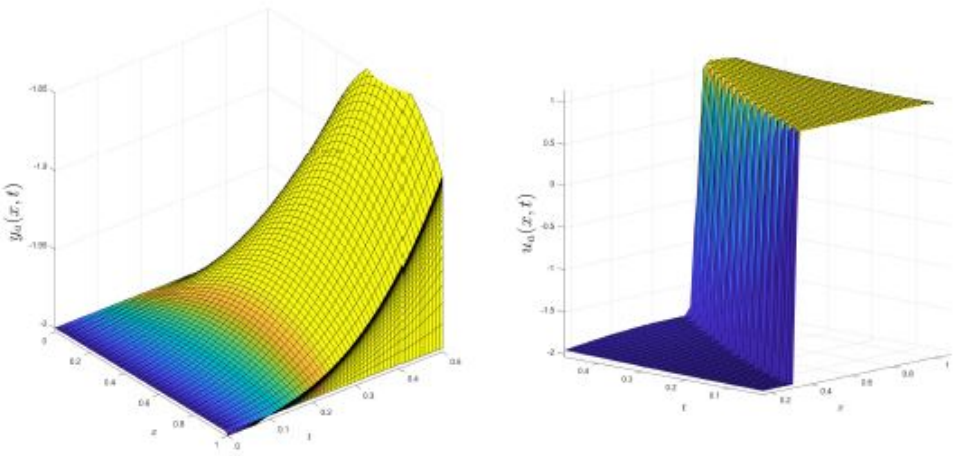

Fig. 1. Surface plot of numerical approximation to y and u with $\varepsilon = 2^{-12}$ and $N = M = 64$ for Example 5.1.

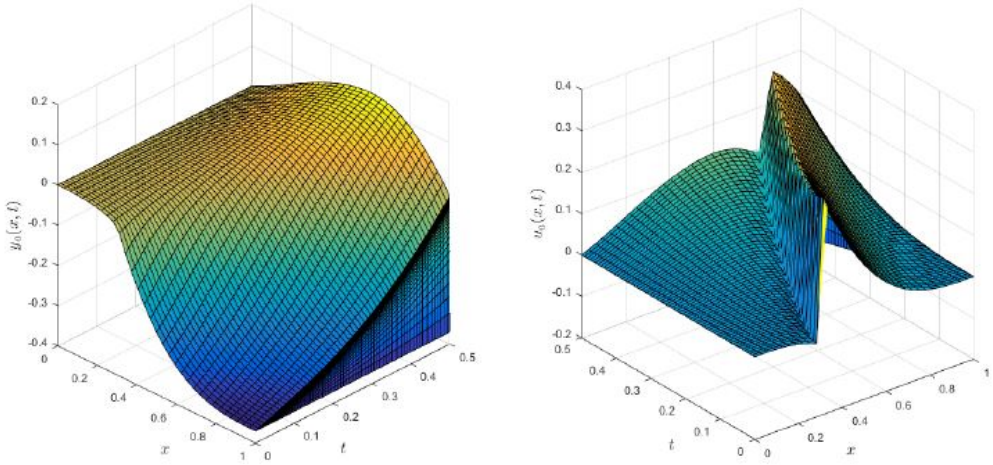

Fig. 2. Surface plot of numerical approximation to y and u with $\varepsilon = 2^{-12}$ and $N = M = 64$ for Example 5.2.

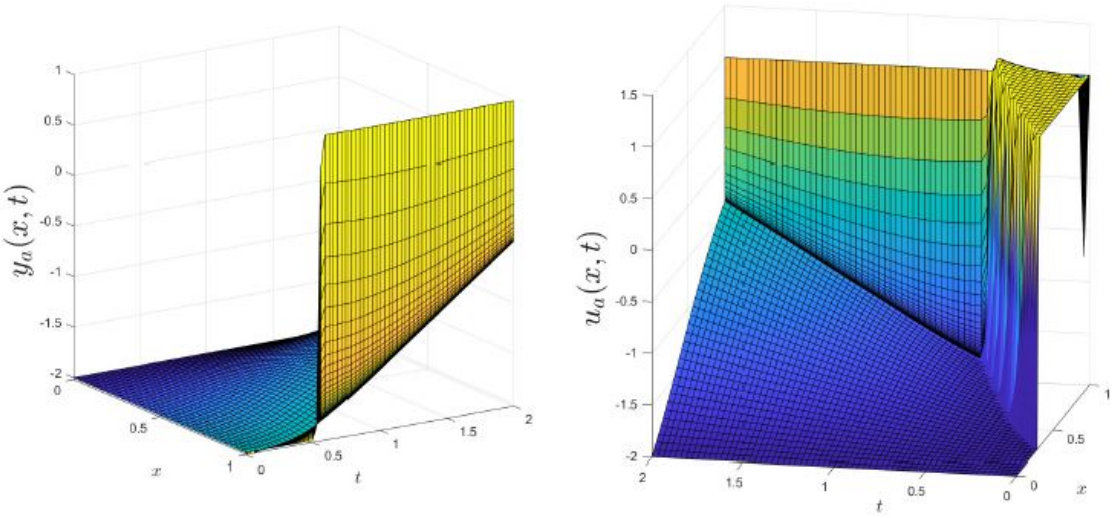

Fig. 3. Surface plot of numerical approximation to y and u with $\varepsilon = 2^{-12}$ and $N = M = 64$ for Example 5.3.

Table 1. Maximum point-wise errors and the corresponding order of convergence for the function y in Example 5.1, computed using the upwind scheme

$\epsilon \downarrow$	Number of Mesh Intervals ($N = M$)					
	32	64	128	256	512	1024
2^{-2}	1.230e-02	5.783e-03	2.798e-03	1.376e-03	6.821e-04	3.396e-04
	1.088	1.048	1.024	1.012	1.006	
2^{-3}	1.673e-02	1.079e-02	5.191e-03	2.547e-03	1.262e-03	6.280e-04
	0.633	1.055	1.027	1.013	1.007	
2^{-4}	2.008e-02	7.991e-03	4.652e-03	2.642e-03	1.484e-03	8.235e-04
	0.776	0.781	0.816	0.832	0.850	
2^{-6}	4.800e-03	2.698e-03	1.557e-03	8.862e-04	4.976e-04	2.763e-04
	0.831	0.792	0.813	0.833	0.848	
2^{-8}	2.468e-03	1.323e-03	7.255e-04	3.993e-04	2.204e-04	1.221e-04
	0.900	0.866	0.862	0.857	0.851	
2^{-10}	2.875e-03	1.679e-03	9.370e-04	5.184e-04	2.860e-04	1.572e-04
	0.776	0.841	0.854	0.858	0.864	
2^{-12}	2.968e-03	1.707e-03	9.543e-04	5.288e-04	2.927e-04	1.612e-04
	0.798	0.839	0.852	0.853	0.861	
2^{-14}	2.992e-03	1.714e-03	9.586e-04	5.313e-04	2.943e-04	1.623e-04
	0.804	0.839	0.851	0.852	0.859	
$\vdots$	$\vdots$	$\vdots$	$\vdots$	$\vdots$	$\vdots$	$\vdots$
2^{-18}	1.368e-03	4.806e-03	2.838e-04	1.632e-04	9.278e-04	5.255e-04
	0.736	0.760	0.798	0.815	0.820	
$E^{N,M}$	**2.008e-02**	**1.079e-02**	**5.191e-03**	**2.642e-03**	**1.484e-03**	**8.235e-04**
$P^{N,M}$	**0.896**	**1.055**	**0.974**	**0.832**	**0.849**	

Table 2. Maximum point-wise errors and the corresponding order of convergence for the function y in Example 5.2, computed using the upwind scheme

$\varepsilon \downarrow$	Number of Mesh Intervals ($N = M$)					
	32	64	128	256	512	1024
2^{-2}	3.590e-03	4.569e-03	3.007e-03	2.481e-03	1.694e-03	1.314e-03
	-0.348	0.603	0.278	0.550	0.367	
2^{-4}	7.415e-03	3.990e-03	2.255e-03	1.247e-03	7.917e-04	6.614e-04
	0.894	0.823	0.854	0.656	0.259	
2^{-6}	1.125e-02	7.051e-03	4.061e-03	2.202e-03	1.154e-03	5.894e-04
	0.674	0.796	0.883	0.933	0.969	
2^{-8}	1.425e-02	9.726e-03	6.373e-03	3.921e-03	2.277e-03	1.248e-03
	0.551	0.610	0.701	0.784	0.8671	
2^{-10}	1.519e-02	1.088e-02	7.564e-03	5.138e-03	3.344e-03	2.063e-03
	0.482	0.524	0.558	0.620	0.697	
2^{-12}	1.543e-02	1.121e-02	7.945e-03	5.636e-03	3.911e-03	2.651e-03
	0.461	0.497	0.495	0.527	0.561	
2^{-14}	1.550e-02	1.130e-02	8.048e-03	5.777e-03	4.102e-03	2.893e-03
	0.456	0.490	0.478	0.494	0.504	
$\vdots$	$\vdots$	$\vdots$	$\vdots$	$\vdots$	$\vdots$	$\vdots$
2^{-18}	1.421e-02	4.806e-02	2.838e-03	1.632e-03	9.278e-03	5.255e-03
	0.736	0.760	0.798	0.815	0.820	
$E^{N,M}$	**1.550e-02**	**1.130e-02**	**8.048e-03**	**5.777e-03**	**4.102e-03**	**2.893e-03**
$P^{N,M}$	**0.455**	**0.489**	**0.478**	**0.494**	**0.503**	

Table 3. Maximum point-wise errors and the corresponding order of convergence for the function y in Example 5.3, computed using the upwind scheme

$\varepsilon \downarrow$	Number of Mesh Intervals ($N = M$)					
	32	64	128	256	512	1024
2^{-2}	4.847e-02	2.486e-02	1.259e-02	6.342e-03	3.182e-03	1.594e-03
	0.963	0.981	0.990	0.995	0.997	
2^{-3}	7.498e-02	5.263e-02	2.677e-02	1.350e-02	6.782e-03	3.399e-03
	0.511	0.975	0.988	0.993	0.996	
2^{-4}	7.313e-02	4.724e-02	2.811e-02	1.670e-02	9.579e-03	5.411e-03
	0.630	0.749	0.751	0.802	0.824	
2^{-6}	6.547e-02	3.302e-02	2.205e-02	1.392e-02	1.154e-03	3.363e-03
	0.987	0.582	0.663	0.708	0.782	
2^{-8}	7.872e-02	4.619e-02	2.731e-02	1.621e-02	9.305e-03	5.274e-03
	0.769	0.758	0.753	0.801	0.819	
2^{-10}	6.44e-02	3.230e-03	2.141e-04	1.35e-04	3.540e-04	1.572e-04
	0.786	0.790	0.793	0.797	0.799	
2^{-12}	7.996e-02	4.778e-02	2.797e-02	1.616e-02	9.278e-03	5.256e-03
	0.743	0.772	0.791	0.801	0.820	
2^{-14}	8.020e-02	4.796e-02	2.821e-02	1.619e-02	9.278e-03	5.256e-03
	0.742	0.765	0.801	0.804	0.820	
$\vdots$	$\vdots$	$\vdots$	$\vdots$	$\vdots$	$\vdots$	$\vdots$
2^{-18}	8.008e-02	4.806e-02	2.838e-02	1.632e-02	9.278e-03	5.255e-03
	0.736	0.760	0.798	0.815	0.820	
$E^{N,M}$	**8.020e-02**	**5.263e-02**	**2.838e-02**	**1.670e-02**	**9.579e-03**	**5.411e-03**
$P^{N,M}$	**0.607**	**0.891**	**0.765**	**0.801**	**0.824**	

Table 4. Maximum point-wise errors and order of convergence for Example 5.1 after extrapolation

$\varepsilon \downarrow$	Number of Mesh Intervals ($N = M$)					
	32	64	128	256	512	1024
2^{2}	1.611e-03	4.072e-04	1.023e-04	2.560e-05	6.401e-06	1.600e-06
	1.984	1.992	1.998	1.999	1.999	
2^{-3}	3.020e-03	7.848e-04	1.982e-04	4.966e-05	1.243e-05	3.108e-06
	1.944	1.985	1.996	1.998	1.999	
2^{-4}	5.205e-03	1.495e-03	3.880e-04	9.793e-05	2.454e-05	6.139e-06
	1.800	1.945	1.986	1.996	1.999	
2^{-6}	3.374e-03	1.902e-03	7.464e-4	1.936e-04	4.886e-05	1.224e-05
	1.499	1.468	1.464	1.496	1.498	
2^{-8}	1.691e-03	1.008e-03	5.089e-04	2.064e-04	7.276e-05	2.583e-05
	1.560	1.564	1.579	1.5941	1.610	
2^{-10}	8.466e-4	5.111e-04	2.568e-04	1.039e-04	3.660e-05	1.301e-05
	1.429	1.454	1.505	1.523	1.612	
2^{-12}	4.236e-04	2.574e-04	1.290e-04	5.215e-05	1.836e-05	6.529e-06
	1.449	1.554	1.520	1.562	1.591	
2^{-14}	2.119e-04	1.292e-04	6.466e-05	2.612e-05	9.193e-06	3.271e-06
	1.481	1.477	1.566	1.5910	1.619	
$\vdots$	$\vdots$	$\vdots$	$\vdots$	$\vdots$	$\vdots$	$\vdots$
2^{-18}	2.650e-05	1.631e-5	9.064e-06	4.682e-6	2.294e-6	1.050e-06
	1.470	1.530	1.594	1.670	1.645	
$E_{extp}^{N,M}$	**3.462e-03**	**3.546e-03**	**1.531e-04**	**4.269e-04**	**2.067e-05**	**1.676e-05**
$P_{extp}^{N,M}$	**1.696**	**1.655**	**1.675**	**1.5644**	**1.6884**	

Table 5. Maximum point-wise errors and order of convergence for Example 5.2 after extrapolation

$\varepsilon \downarrow$	Number of Mesh Intervals ($N = M$)					
	32	64	128	256	512	1024
2^{-2}	5.205e-03	1.495e-03	3.880e-04	9.793e-05	2.454e-05	6.139e-06
	1.944	1.985	1.996	1.998	1.999	
2^{-3}	3.020e-03	7.848e-04	1.982e-04	4.966e-05	1.243e-05	3.108e-06
	1.469	1.515	1.546	1.573	1.589	
2^{-4}	5.205e-03	1.495e-03	3.88e-04	9.796e-05	2.454e-05	6.139e-06
	1.80	1.94	1.98	1.99	1.99	
2^{-6}	1.0447e-02	3.7506e-02	1.0048e-02	4.5245e-03	1.0753e-03	1.224e-05
	1.477	1.573	1.590	1.630	1.621	
2^{-8}	1.0958e-02	3.5297e-02	1.1075e-02	3.5655e-03	1.0740e-03	2.583e-05
	1.6344	1.6722	1.6352	1.7310	1.781	
2^{-10}	1.0450e-02	3.7503e-02	1.2169e-02	4.0518e-03	1.3059e-03	1.301e-05
	1.4784	1.538	1.586	1.633	1.674	
2^{-12}	1.0450e-02	3.7502e-02	1.3203e-02	3.5649e-03	1.3059e-03	6.529e-06
	1.4784	1.5061	1.5890	1.588	1.599	
2^{-14}	1.0450e-02	3.9415e-02	1.0040e-02	4.5270e-03	1.3059e-03	3.271e-06
	1.4067	1.573	1.591	1.595	1.598	
$\vdots$	$\vdots$	$\vdots$	$\vdots$	$\vdots$	$\vdots$	$\vdots$
2^{-18}	1.0450e-02	3.7502e-02	1.1075e-02	4.0518e-03	1.9342e-03	3.271e-06
	1.4784	1.567	1.576	1.568	1.598	
$E_{extp}^{N,M}$	**3.462e-02**	**3.546e-02**	**1.531e-03**	**4.269e-04**	**1.676e-05**	**2.067e-05**
$P_{extp}^{N,M}$	**1.425**	**1.587**	**1.594**	**1.681**	**1.694**	

Table 6. Maximum point-wise errors and order of convergence for Example 5.3 after extrapolation

$\varepsilon \downarrow$	Number of Mesh Intervals ($N = M$)					
	32	64	128	256	512	1024
2^{-2}	1.039e-02	3.482e-02	1.077e-02	4.176e-03	1.358e-03	1.527e-04
	1.577	1.692	1.367	1.620	1.651	
2^{-3}	1.0411e-02	3.760e-02	1.315e-02	4.503e-03	1.108e-03	1.334e-04
	1.4691	1.5152	1.5466	1.567	1.631	
2^{-4}	1.043e-02	3.752e-02	1.318e-02	4.518e-03	1.308e-03	1.33e-04
	1.476	1.508	1.545	1.631	1.683	
2^{-6}	1.044e-02	3.750e-2	1.004e-2	4.5245e-3	1.075e-3	1.637e-04
	1.477	1.503	1.510	1.630	1.652	
2^{-8}	1.095e-02	3.529e-02	1.107e-02	3.565e-03	1.074e-03	1.64e-04
	1.634	1.672	1.635	1.731	1.781	
2^{-10}	1.045e-02	3.750e-02	1.216e-02	4.051e-03	1.305e-03	1.450e-04
	1.478	1.523	1.586	1.633	1.671	
2^{-12}	1.045e-02	3.750e-2	1.320e-02	3.564e-03	1.305e-03	1.613e-04
	1.4784	1.5061	1.589	1.648	1.687	
2^{-14}	1.045e-02	3.941e-2	1.004e-2	4.527e-3	1.305e-3	1.35e-04
	1.406	1.473	1.494	1.495	1.498	
$\vdots$	$\vdots$	$\vdots$	$\vdots$	$\vdots$	$\vdots$	$\vdots$
2^{-18}	1.045e-02	3.750e-02	1.107e-02	4.051e-03	1.934e-03	1.343e-04
	1.478	1.451	1.456	1.466	1.489	
$E^{N,M}_{extp}$	**1.0958e-02**	**3.9415e-02**	**1.3203e-02**	**4.5270e-03**	**1.9342e-03**	1.931e-04
$P^{N,M}_{extp}$	**1.425**	**1.587**	**1.594**	**1.681**	**1.698**	

5.2 Improvement of the solution using Richardson extrapolation technique

In our MATLAB computations, we implemented the Richardson extrapolation scheme to achieve higher-order convergence in the numerical method.

To solve the SPPCDP in Examples 5.1, 5.2, and 5.3, we employ the upwind finite difference method for spatial derivatives and the implicit-Euler strategy for temporal derivatives on two meshes ($E^{N,M}$ and $E^{2N,2M}$). Here, the data provided that by using upwind finite difference scheme table 1, 2, and 3 presents the maximum error and order of convergence, then we obtain almost first-order convergence rate.

The numerical solution for the model problem (2.1) is then computed on two interconnected meshes, yielding a second-order convergent solution per (4.4).

In addition, tables 4, 5, and 6 clearly show the effectiveness of Richardson extrapolation in increasing the order of convergence of the upwind method. Similarly, tables 4, 5, and 6 show that extrapolation improves the numerical solution of the convergence rate from $O(N^{-1}\ln N)$ to $O(N^{-2}\ln^2 N)$ for $\Delta t = 1/N$. This result is compatible with the theoretical constraints stated in Theorem 3.3. These tables indicate our ability to precisely identify maximum pointwise errors and convergence rates for Examples 5.1, 5.2, and 5.3, indicating almost second-order convergence.

6 Conclusions

This article examines the use of Richardson extrapolation to solve singularly perturbed parabolic convection-diffusion problems with DIC (2.1). First, we use the piecewise-uniform Shishkin mesh to discretize the domain, and then we use implicit Euler for time discretization on a uniform mesh and an upwind finite difference method for spatial discretization. The obtained results demonstrate an approximate first-order convergence rate for the upwind method. By applying Richardson extrapolation, we achieve enhanced accuracy, leading to an approximate second-order convergence rate. The convergence rate increases as ε increases from $O\left(N^{-1}\ln N + \Delta t\right)$ to $O\left(N^{-2}\ln^2 N + \Delta t^2\right)$, resulting in more reliable and precise solutions with lower node errors. The technique

achieves ε-uniform convergence with second-order accuracy with a modest logarithmic computational component. Tables 1, 2, and 3 offer precise estimates of maximum pointwise errors and convergence rates for Examples 5.1, 5.2, and 5.3, indicating almost first-order convergence. In addition, tables 4, 5, and 6 clearly show the effectiveness of Richardson extrapolation in increasing the order of convergence of the upwind method.

The numerical experiments conducted on three test problems substantiate the theoretical findings. Finally, we implement the Richardson extrapolation technique by combining solutions obtained on N and $2N$ mesh intervals. This amalgamation yields Richardson extrapolations that provide almost second-order uniform convergence approximations

Acknowledgement

The authors are grateful to the referees for their careful reading, constructive criticisms, comments and suggestions, which have helped us to improve this work significantly.

Competing Interests

Author has declared that no competing interests exist.

References

[1] Bobisud L. Parabolic equations with a small parameter and discontinuous data. Journal of Mathematical Analysis and Applications. 1969;26:208-220.

[2] Hemker P, Shishkin G. Discrete approximation of singularly perturbed parabolic pdes with a discontinuous initial condition. in Bail VI Proceedings. 1994;3-4.

[3] O'Riordan E, Shishkin G. Singularly perturbed parabolic problems with non-smooth data. Journal of Computational and Applied Mathematics. 2004;166:233-245.

[4] Sodano D. An upwind finite difference method to singularly perturbed parabolic convection diffusion problems with discontinuous initial conditions on a piecewise-uniform mesh. Mendeley Data. 2024;V2.

[5] Gracia J, O'Riordan E. Numerical approximation of solution derivatives of singularly perturbed parabolic problems of convection-diffusion type. Mathematics of Computation. 2016;85:581-599.

[6] Gracia JL, O'Riordan E. Parameter-uniform approximations for a singularly perturbed convection-diffusion problem with a discontinuous initial condition. Applied Numerical Mathematics. 2021;162:106-123.

[7] Clavero C, Jorge J, Lisbona F. A uniformly convergent scheme on a nonuniform mesh for convection–diffusion parabolic problems. Journal of Computational and Applied Mathematics. 2003;154:415-429.

[8] Gracia JL, O'Riordan E. Singularly perturbed reaction–diffusion problems with discontinuities in the initial and/or the boundary data. Journal of Computational and Applied Mathematics. 2020;370:112638.

[9] Gracia JL, O'Riordan E. Numerical approximations to a singularly perturbed convection-diffusion problem with a discontinuous initial condition. Numerical Algorithms. 2021;88:1851-1873.

[10] Farrell P, Hegarty A, Miller J, O'Riordan E, Shishkin G. Singularly perturbed convection–diffusion problems with boundary and weak interior layers. Journal of Computational and Applied Mathematics. 2004;166:133-151.

[11] Farrell P, Hegarty A, Miller JM, O'Riordan E, Shishkin GI. Robust computational techniques for boundary layers. CRC Press; 2000.

[12] Miller J, O'Riordan E, Shishkin G, Kellogg RB. Fitted numerical methods for singular perturbation problems. SIAM Review. 1997;39:535-537.

[13] Roos HG, Stynes M, Tobiska L. Robust numerical methods for singularly perturbed differential equations: Convection-diffusion-reaction and flow problems. Springer. Science Business Media. 2008;24.

[14] Miller J, O'Riordan E, Shishkin G, Shishkina L. Fitted mesh methods for problems with parabolic boundary layers. in Mathematical Proceedings of the Royal Irish Academy. JSTOR. 1998;173-190.

[15] Clavero C, Gracia JL, Shishkin GI, Shishkina LP. An efficient numerical scheme for 1d parabolic singularly perturbed problems with an interior and boundary layers. Journal of Computational and Applied Mathematics. 2017;318:634-645.

[16] Miller JJ, O'riordan E, Shishkin GI. Fitted numerical methods for singular perturbation problems: Error estimates in the maximum norm for linear problems in one and two dimensions. World Scientific; 1996.

[17] Shishkin GI. Grid approximation of singularly perturbed parabolic convection-diffusion equations with a piecewise-smooth initial condition. Zhurnal Vychislitel'noi Matematiki i Matematicheskoi Fiziki. 2006;46:52-76.

[18] Shishkin GI. The Richardson scheme for the singularly perturbed parabolic reaction-diffusion equation in the case of a discontinuous initial condition. Computational Mathematics and Mathematical Physics. 2009;49:1348-1368.

[19] Gracia J, O'Riordan E. A singularly perturbed convection–diffusion problem with a moving interior layer. Int. J. Numer. Anal. Model. 2012;9:823-843.

[20] O'Riordan E, Pickett M, Shishkin G. Parameter-uniform finite difference schemes for singularly perturbed parabolic diffusion-convection-reaction problems. Mathematics of Computation. 2006;75:1135-1154.

[21] Doolan EP, Miller JJ, Schilders WH. Uniform numerical methods for problems with initial and boundary layers. Boole Press; 1980.

[22] Lozano JLG, Gracia CC. Richardson extrapolation on generalized shishkin meshes for singularly perturbed problems. in VIII Journ´ees Zaragoza-Pau de Math´ematiques Appliqu´ees et de Statistiques, Prensas de la Universidad de Zaragoza. 2003;169-178.

[23] Natividad MC, Stynes M. Richardson extrapolation for a convection–diffusion problem using a shishkin mesh. Applied Numerical Mathematics. 2003;45:315-329.

[24] Shishkin G. Robust novel high-order accurate numerical methods for singularly perturbed convection-diffusion problems. Mathematical Modelling and Analysis. 2005;10:393-412.

[25] Shishkin G, Shishkina L. The richardson extrapolation technique for quasilinear parabolic singularly perturbed convection-diffusion equations. in Journal of Physics: Conference Series, IOP Publishing. 2006;55:203.

[26] Clavero C, Gracia J, Jorge J. High-order numerical methods for one-dimensional parabolic singularly perturbed problems with regular layers. Numerical Methods for Partial Differential Equations: An International Journal. 2005;21:149-169.

[27] Munyakazi JB, Patidar KC. On richardson extrapolation for fitted operator finite difference methods. Applied Mathematics and Computation. 2008;201:465-480.

[28] Linss. Layer-adapted meshes for reaction-convection-diffusion problems. Springer; 2009.

[29] Yadav NS, Mukherjee K. On -uniform higher order accuracy of new efficient numerical method and its extrapolation for singularly perturbed parabolic problems with boundary layer. International Journal of Applied and Computational Mathematics. 2021;7:72.

[30] Dunne RK, O'Riordan E, Shishkin GI. A fitted mesh method for a class of singularly perturbed parabolic problems with a boundary turning point. Computational Methods in Applied Mathematics. 2003;3:361-372.

[31] Keller HB. Numerical methods for two-point boundary-value problems. Courier Dover Publications; 2018.

[32] Linß T. An upwind difference scheme on a novel shishkin-type mesh for a linear convection– diffusion problem. Journal of Computational and Applied Mathematics. 1999;110:93-104.

[33] Stynes M, Roos HG. The midpoint upwind scheme. Applied Numerical Mathematics. 1997;23:361-374.

Peer-review history:
The peer review history for this paper can be accessed here (Please copy paste the total link in your browser address bar)
https://prh.globalpresshub.com/review-history/1463